

## FURTHER INVESTIGATIONS OF SEMICONDUCTIVITY AND PYROELECTRICITY FOR THE DEVELOPMENT OF POLED AND Cd-DOPED MERCURY TELLURIDE THIN FILM IN ELECTRONICS AND ENGINEERING

M.M. ABOU SEKKINA \*, A. TAWFIK and M.I. ABD EL-ATI

*Faculty of Science, Tanta University, Tanta (Egypt)*

(Received 18 July 1984)

### ABSTRACT

The crystalline structure, electrical conductivity and pyroelectricity of developed mercury telluride thin films have been investigated in detail. Analysis of data obtained confirms that these properties are in agreement. Consequently, the role of Hg migration, non-stoichiometry, diffusion of impurities and degree of crystallinity are clearly cut. Finally, the optimum conditions were evaluated and recommended for mercury telluride thin films in electronic industries and engineering.

### INTRODUCTION

It is of interest to note that HgTe and thus CdTe have the zinc blende structure and form a continuous series of alloys [1–3] denoted by  $\text{Hg}_{(1-x)}\text{Cd}_x\text{Te}$ , where  $x$  is the mole fraction of Cd in the alloy. These alloys are a mixture of a semimetal (HgTe) with a semiconductor (CdTe); the energy gap,  $E_G$ , in these alloys varies continuously [4,5] between the “negative gap” ( $-0.30$  eV) [6] found in HgTe to the positive gap (1.60 eV) [7,8] found in CdTe. Narrow-gap semiconducting alloys in this system have proved useful as IR detectors [9].

In the last 10–15 years the study of the electrophysical and structural properties of thin film semiconducting materials has been intensified due to its increasing number of applications in electronics, optics, solar cells, radiation dosimetry, opto-electronics and energetics.

The present investigation was carried out to evaluate the effects of either poling or Cd-doping on the structural, electrical and pyroelectric properties of an HgTe thin film with an attempt to attain the optimum conditions for its final application in electronics and solar cell devices.

---

\* Author to whom correspondence should be addressed.

## EXPERIMENTAL

*Material synthesis*

HgTe and CdTe were prepared by direct melting of equimolecular ratios of the two component elements under vacuum ( $10^{-5}$  mm Hg) in quartz capsules [10]. Their phase constitutions were identified by means of X-ray diffraction analysis. From these two materials, a thin film of HgCdTe was obtained by thermal evaporation of 43.4 mg of the well-prepared CdTe and the same amount of the well-prepared HgTe materials in a coating unit (Edward, England) under vacuum ( $6 \times 10^{-5}$  mm Hg), at a temperature of  $100^\circ\text{C}$  on glass substrate. The evaporation temperature was  $800^\circ\text{C}$ . The thickness of the thin film obtained was found to be  $0.5 \mu\text{m}$  using an interference microscope. The components used were of pure analytical grade (99.98%).

*X-ray diffraction measurements*

The crystalline structures of the prepared  $\text{Hg}_{0.7}\text{Cd}_{0.3}\text{Te}$  thin film were conducted before and after heating using a Shimadzu (Japan) X-ray diffractometer,  $\text{Cu } K_\alpha$  radiation and Ni filter.

*DC electrical resistivity and I-V characteristic measurements*

These were undertaken using an Orion (Budapest) electrometer (type TR-1501) at room and elevated temperatures and various applied voltages.

*Sample poling and pyroelectric measurements*

Poling was carried out in silicon oil at varying temperatures up to  $120^\circ\text{C}$  and under an applied voltage of 300 V. The sample was then cooled to room temperature with the field maintained throughout, at a cooling rate of  $2.5^\circ\text{C min}^{-1}$ .

The pyroelectric current generated was measured with an Orion (Budapest) electrometer (type TR-1501).

## RESULTS AND DISCUSSION

Figure 1 and Table 1 show the  $\text{Cu } K_\alpha$ , relative intensity ( $I/I_0$ ) and interplanar spacings of the characteristic X-ray diffractograms of unheated (A,  $20^\circ\text{C}$ ) and preheated (B,  $150^\circ\text{C}$ ) HgCdTe thin films. From the results obtained it can be easily seen that the X-ray diffraction peaks have a common general trend, namely, the deflection peaks sharpen and their

TABLE 1

Analysis of the obtained Cu  $K_{\alpha}$  X-ray diffraction patterns of unheated and preheated (150°C)  $\text{Hg}_{0.70}\text{Cd}_{0.30}\text{Te}$  thin films

Serial No.	(A) Unheated thin film			(B) Preheated (150°C) film		
	$2\theta^{\circ}$	$d(\text{\AA})$	$I/I_0$	$2\theta^{\circ}$	$d(\text{\AA})$	$I/I_0$
1	9.70	9.1103	1	11.2	7.8933	1
2	13.40	6.6019	1	14.54	6.0868	1
3	15.40	5.7487	1	15.93	5.5691	2
4	18.10	4.8968	2	16.70	5.3040	2
5	18.60	4.7663	3	22.30	3.9831	4
6	21.00	4.2267	3	23.24	3.8241	18
7	21.60	4.1106	4	26.90	3.3115	4
8	23.00	3.8635	19	29.00	3.0769	5
9	25.00	3.5587	2	32.4	2.7608	100
10	27.00	3.2995	3	34.5	2.5974	8
11	29.10	3.0668	7	38.70	2.3247	5
12	32.24	2.7742	100	39.90	2.2575	4
13	34.60	2.6300	6	46.10	1.9673	1
14	38.00	2.3659	4	49.10	1.8538	1
15	38.60	2.3305	4			
16	39.90	2.2575	3			
17	41.00	2.1994	1			
18	46.24	1.9616	2			

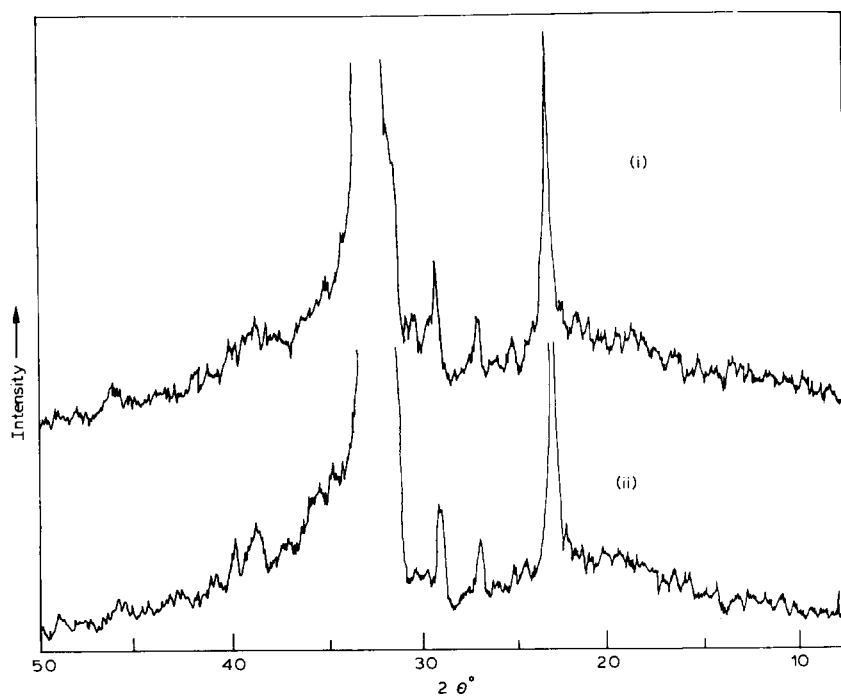


Fig. 1. X-ray diffraction patterns of  $\text{Hg}_{0.7}\text{Cd}_{0.3}\text{Te}$  vacuum-evaporated thin films: (i) unheated sample; (ii) sample preheated at 150°C.

TABLE 2

The activation energies and energy gaps (eV) obtained for a Cd-modified HgTe thin film under 15 and 20 V applied voltages

(A) 15 volts		(B) 20 volts	
Activation energy (eV)	Energy gap (eV)	Activation energy (eV)	Energy gap (eV)
0.2	0.10	0.03	0.10
0.08	—	0.08	—

intensities are increased by preheating the thin film at 150°C. This could be correlated with the further crystallization and increased degree of crystallinity together with cubic structure improvements. This indicates that the number of non-stoichiometrical atoms or non-stoichiometry decreases and the degree of crystallinity increases for the preheated sample (150°C).

Figure 2 shows the variation of logarithmic electrical conductivity vs. the reciprocal of the absolute temperature ( $1000/T$ ) using applied voltages of 15 (curve A) and 20 V (curve B).

The composition was chosen to evaluate the effect of Hg migration and non-stoichiometry on the electrical characteristics of the test sample. In each plot, there are two temperature intervals in which the charge carrier concentrations show a different dependence on temperature. This behaviour is often observed in semiconductor compounds. The lower, and the higher,

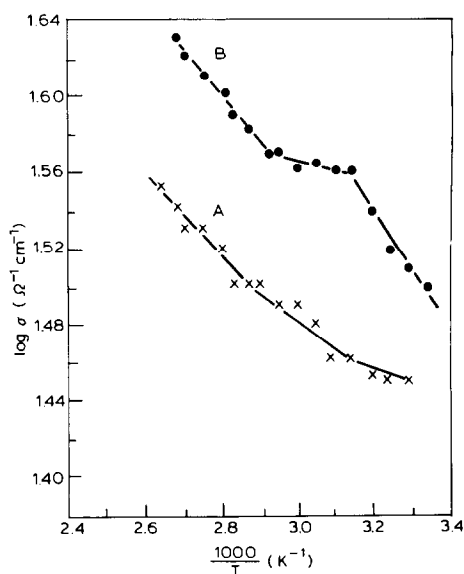


Fig. 2. Variation of logarithmic electrical conductivity as a function of reciprocal temperature: (A) applied field = 15 V; (B) applied field = 20 V.

temperature portions vary exponentially according to the well-known relation [11]

$$\sigma = \sigma_0 e^{-\Delta E/2KT}$$

From this relation, the activation energy for the process of electrical conduction was calculated in the low and high temperature regions (eV), as shown in Table 2.

From Fig. 2, it can be easily seen that the electrical conductivity considerably increases with voltage from 15 to 20 V (curves A and B, respectively). This could probably be correlated with the improved mobilization of Hg to the edges of crystallites under 20 V than under 15 V.

Thus, mercury migration may lead to a decreased potential barrier between the crystallites. Again, the observed increase in activation energy at higher temperatures gives further support to the idea of passing from extrinsic to intrinsic conduction mechanisms (Fig. 2). Since the high temperature activation energy remains constant (0.01 eV), this therefore corresponds to the intrinsic conduction mechanism as well as to an energy gap of the test specimen. For the relatively low temperature region, the activation energies could be accounted for by an extrinsic conduction mechanism. This is further supported by the fact that their values are interchangeable, due to changes in the course of the heat treatment to which the specimen is subjected and/or migration of Hg from the bulk of materials to the crystallite edges.

A typical I-V characteristic curve is shown in Fig. 3, which is ohmic up to ~ 20 V. The current at low field varies with temperature in accordance with

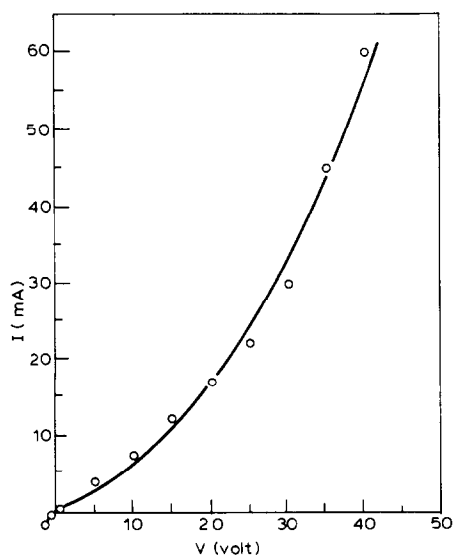


Fig. 3. Typical I-V characteristic curve for the  $\text{Hg}_{0.7}\text{Cd}_{0.3}\text{Te}$  thin film investigated.

the equation [12]

$$I_c = I_0 \exp(-\Delta E/2KT) \quad (2)$$

where  $\Delta E$  is the activation energy for donors or traps and

$$I_0 \equiv q\mu N_d \frac{V_b}{d} A \quad (3)$$

where  $q$  is the electronic charge,  $\mu$  is the mobility,  $N_d$  is the impurity density,  $V_b$  is the bias voltage,  $d$  is the effective electrode separation and  $A$  is the effective area. Normally, the current carrier in this material is of electronic and/or hole type. It is known that Hg/Cd and Te are weakly bound through intermetallic bonds. Thus, it was first suggested that the non-linearity in the  $I$ - $V$  curve of this compound is due to the space charge of un-neutralized carriers [13] when a relatively high electric field (300 V as a poling field) is applied. The non-linearity in the  $I$ - $V$  above 20 V (Fig. 3) is due to the domain structure of the material investigated. Thus, the onset of non-linear conduction would create such high current and power densities that power dissipation under continuous operation is destructive [14]. A plot of  $\log I_c$  against  $1000/T$  according to eqn. (2) yields variable slopes. The gradients of these slopes yield a consistent value for the activation energy ( $\Delta E = 0.1$  eV) at different voltages (15 and 20 V). Using  $N_d$  (in eqn. 3)  $\approx 6 \times 10^{18} \text{ cm}^{-3}$ , the mobility was estimated to be  $1.28 \times 10^{-2} \text{ cm}^2 \text{ V}^{-1} \text{ s}^{-1}$ . These relatively low values of mobility and activation energy with an ohmic

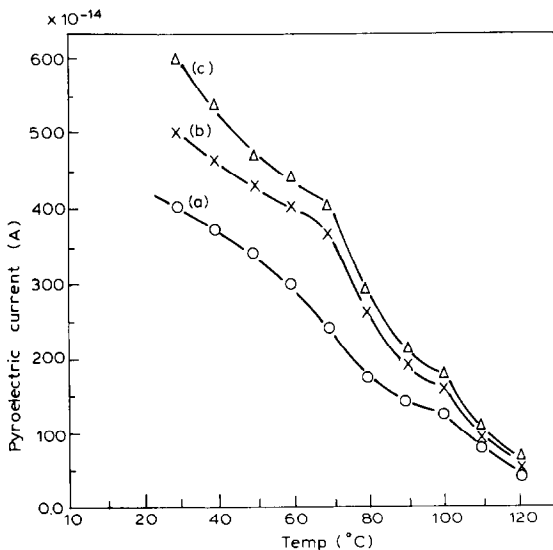


Fig. 4. Diagrammatical representation of the variation of the generated pyroelectric current (A) as a function of temperature ( $^{\circ}\text{C}$ ) at different heating rates: (a)  $2^{\circ}\text{C min}^{-1}$ ; (b)  $5^{\circ}\text{C min}^{-1}$ ; (c)  $10^{\circ}\text{C min}^{-1}$ .

$I_c-V_c$  characteristic ( $\sim 20$  V) are an indication of a localized state conduction (hopping) at relatively low field and high temperature. Consequently, the estimated hopping mobility of  $1.28 \times 10^{-2} \text{ cm}^{-1} \text{ V}^{-1} \text{ s}^{-1}$  is associated with a 0.01 eV activation energy at higher temperature (see Fig. 2 and Table 2). The break-through voltage is inversely proportional to the donor density and the density of surface states. Accordingly, these features are important in the fabrication of micro-electronic circuits.

Figure 4 illustrates the variation of pyroelectric current (A) as a function of temperature at various heating rates ( $2, 5$  and  $10^\circ\text{C min}^{-1}$  for curves a, b and c, respectively). From this figure, it can be easily deduced that a higher generated pyroelectric current could be obtained by increasing the heating rate. This could be explained by the action of the heating rate in accelerating the mobilization of Hg to the edges of crystallites leading to a greater accumulation of pyroelectric charges at the surface of the specimen and/or diffusion of impurities.

Figure 5 includes the variation of generated pyroelectric current as a function of poling temperature ( $^\circ\text{C}$ ) at various working temperatures of  $30^\circ\text{C}$  (curve a) and  $100^\circ\text{C}$  (curve b). Both curves are characterized by an initial rise in the pyroelectric current with poling temperature with a rate dependent on the experimental temperature (working) leaving behind a peak value situated at constant temperature ( $T_c$ ). This critical temperature ( $T_c$ ) could probably be ascribed to some kind of change in the electronic band structure of the specimen under investigation. This promotes the conclusion that  $70^\circ\text{C}$  as poling temperature and  $30^\circ\text{C}$  as final working temperature are the optimum conditions for attaining maximum pyroelectric current. Thus, in conformity with the X-ray data (see Fig. 1 and Table 1), the increased degree

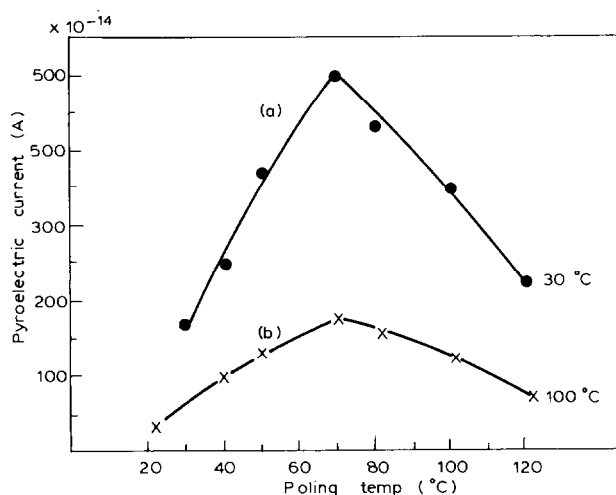


Fig. 5. Variation of the generated pyroelectric current (A) as a function of poling temperature at different working temperatures: (a)  $30^\circ\text{C}$ ; (b)  $100^\circ\text{C}$ .

of crystallinity (for sample preheated at 150°C) will offer an additional resistance or barrier energy for pyroelectric charge release.

Accordingly, results of X-ray diffraction analysis are in agreement with results of pyroelectric measurements.

Figure 6 represents the variation of pyroelectric current as a function of temperature at various poling temperatures. At the initial heating stages, the pyroelectric current slowly falls, followed by a sudden decrease, corresponding to breaks in the curves, at temperatures dependent on the poling temperature.

The results obtained display that the maximum generated pyroelectric current is attained with 70°C as the poling temperature. On the other hand, a 70°C poling temperature causes the investigated thin film to withstand relatively high temperatures up to 70°C after which a sudden drop in the pyroelectric current occurs. For the other poling temperatures, the thin films investigated suffered a sudden low temperature drop in the generated pyroelectric current (40 and 50°C) for samples poled at 20 and 120°C.

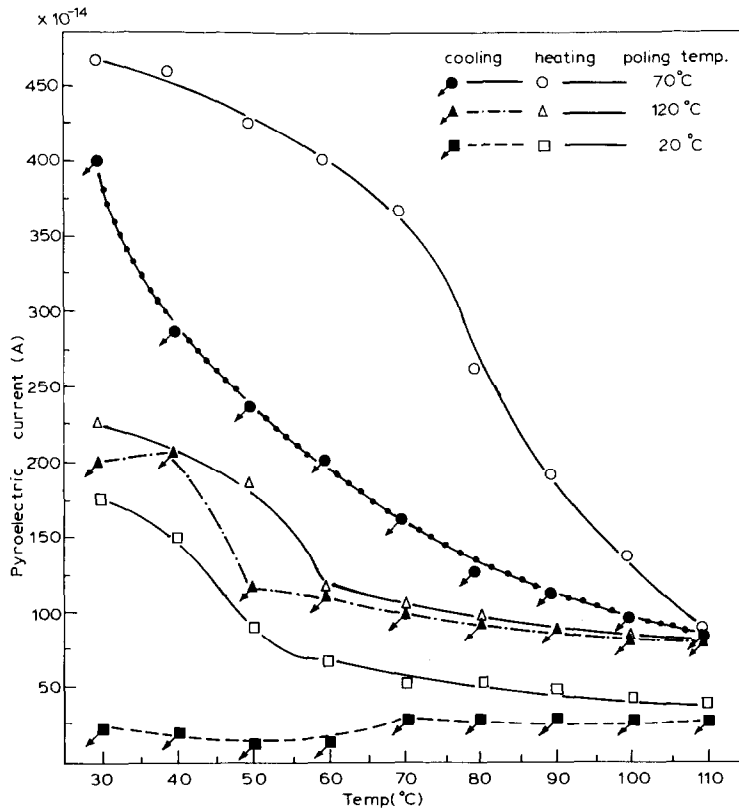


Fig. 6. Variation of the generated pyroelectric current (A) as a function of temperature at various poling temperatures, and on cooling.



respectively.

Alternatively, a 70°C poling temperature constitutes the best poling temperature for attaining a high generated pyroelectric current withstanding relatively high working temperatures for the investigated HgCdTe thin films in electronic industries and engineering.

## REFERENCES

- 1 W.D. Lawson, S. Nielson, E.H. Putley and A.S. Young, *J. Phys. Chem. Solids*, 9 (1959) 325.
- 2 J.L. Schmit and C.J. Speerschneider, *Infrared Phys.*, 8 (1968) 247.
- 3 D. Long, *Energy Band in Semiconductors*, Wiley, New York, 1968, p. 156.
- 4 I. Mclingailis and A.J. Strauss, *Appl. Phys. Lett.*, 8 (1966) 179.
- 5 M.W. Scott, *J. Appl. Phys.*, 40 (1969) 4077.
- 6 C.R. Pidgeon and S. Groves, in D.G. Thomas (Ed.), *Proc. Int. Conf. on II-VI Semiconducting Compounds*, Benjamin, New York, 1967, p. 1980.
- 7 D.G. Thomas, *J. Appl. Phys.*, 32 (1961) 2298.
- 8 W.G. Spitzer and C.A. Mead, *J. Phys. Chem. Solids*, 25 (1964) 443.
- 9 D. Long and J.L. Schmidt, in R.K. Willardson and A.C. Beer (Eds.), *Semimetals and Semiconductors*, Academic Press, New York, 1970, Vol. 5, Chap. 5.
- 10 Z.M. Hanafi, K.A. Alzweil, E.M.H. Ibrahim and M.M. Abou Sekkina, *Z. Phys. Chem., Neue Folge* (1975) 291.
- 11 K.A. Alzweil, M.M. Abou Sekkina and Z.M. Hanafi, *Z. Phys. Chem. Neue Folge*, (1975) 235.
- 12 S.A.Y. Al-Ismail and C.A. Hogarth, *J. Mater. Sci.*, 18 (1983) 2777.
- 13 A. Tawfik, M.M. Abou Sekkina and N.A. Molokhia, *Sprechsaal*, 12 (1980) 946.
- 14 W. Beam, *Electronics of Solids*, McGraw-Hill, New York, 1965, p. 211.